Briefings in Bioinformatics
doi.10.1093/bioinformatics/xxxxxx
Advance Access Publication Date: Day Month Year
Manuscript Category

OXFORD

Subject Section

Incremental modelling and analysis of hypercholesterolemia therapy with fuzzy hybrid Petri nets

George Assaf [1], Fei Liu [2,*] and Monika Heiner [1]

[1]Department of Computer Science, Brandenburg University of Technology Cottbus-Senftenberg, Cottbus 03046, Germany, and [2]School of Software Engineering, South China University of Technology, Guangzhou 510006, P.R. China.

*To whom correspondence should be addressed.

Associate Editor: XXXXXXX

Received on XXXXX; revised on XXXXX; accepted on XXXXX

Abstract

Modelling biological systems depends on the availability of data and components of the system at hand. With the enhancement of knowledge of a system's data and components, the appropriate modelling paradigm can be adopted to incrementally model and analysis the system's behaviour. However, there is a lack in methodology and tool support for incrementally modelling and analysing biological systems in an intuitive manner. In this paper, we employ fuzzy hybrid Petri net as a powerful expressive tool for incrementally modelling and analysing different aspects of the cholesterol and lipoprotein metabolism and the therapy of elevated levels of cholesterol as a case study. In this context, quantitatively modelling and analysing the cholesterol and lipoprotein metabolism are crucial for understanding how cholesterol levels are regulated and thus contribute to the therapy of human diseases associated with elevated levels of cholesterol. Whilst ordinary differential equations have been utilised to develop mechanistic models and numerically analyse the cholesterol metabolism, modelling the therapy requires capturing discrete events to be integrated into the deterministic system. Moreover, modelling biological systems including cholesterol metabolism lacks complete knowledge of kinetic data calling for means to cope with the resulting uncertainty in model behaviour. The incremental modelling and analysis approach with fuzzy hybrid Petri nets presented in this paper can be equally applied to many other biological systems.
Contact: george.assaf@b-tu.de,feiliu@scut.edu.cn,monika.heiner@b-tu.de

1 Introduction

With the increasing wealth of knowledge and data on biological systems, we now have the ability to construct and refine models of these systems in an incremental modelling way, i.e. taking advantage of existing validated models and then flexibly adding new components to achieve distinct analysis purposes. Currently, only a few modelling methods and tools can support incremental modelling for biological systems because different biological components may be represented with different modelling formalisms, such as deterministic, stochastic, or uncertain formalisms [1, 2, 3]. Among these, tools like *Matlab* [4] stand out for their powerful representation capabilities. However, *Matlab* can be challenging for computational biologists with limited programming backgrounds to be utilised effectively. In this context, fuzzy hybrid Petri nets ($\mathcal{FHPN}$) [5], as a tool with a graphical user interface, greatly facilitate the process of incremental modelling of biological systems.

$\mathcal{FHPN}$ [3, 5] are a quantitative version of place/transition nets [6] offering a convenient graphical way for representing biological processes with deterministic and stochastic behaviours [7, 8, 9]. Crucially, $\mathcal{FHPN}$ are characterised by their fuzzy techniques to model and analyse kinetic data uncertainties stemming from imprecise knowledge of kinetic data of the modelled system, which is commonly the case in biological systems [10, 11]. $\mathcal{FHPN}$ outperform other types of quantitative Petri nets such as stochastic Petri nets ($\mathcal{SPN}$) [12] and continuous Petri nets ($\mathcal{CPN}$) [13, 14] by their expressive power, as they offer various types of

modelling elements for describing different aspects of biological systems by combing $\mathcal{SPN}$, $\mathcal{CPN}$, and fuzzy modelling in one net class.

$\mathcal{FHPN}$ offer an excellent tool for incremental modelling by incorporating step-wise new components into an $\mathcal{FHPN}$ model for describing either stochastic, deterministic or fuzzy aspects of a given biological system. In this paper, we present an incremental modelling approach that can be adopted to a wide range of biological systems. For this purpose we use a case study, namely *cholesterol and lipoprotein metabolism and the therapy of elevated levels of cholesterol* to demonstrate how $\mathcal{FHPN}$ are utilised to achieve incremental modelling of a biological system, which could offer a guideline for incrementally constructing biological models by utilising the existing validated components.

This paper is organised as follows. The next section (Section 2) summarises our methodologies including hybrid Petri nets ($\mathcal{HPN}$) together with their formal definitions and simulation techniques. Thereafter, we describe fuzzy logic and its techniques to cope with the kinetic data uncertainty using $\mathcal{FHPN}$. In Section 3, we present our incremental modelling approach using $\mathcal{FHPN}$ and subsequently, we present the cholesterol metabolism from a biological point of view. This is followed by incremental $\mathcal{FHPN}$ models describing various modelling aspects of the case study. We conclude with a comprehensive discussion in Section 4.

2 Materials and methods

In pursuit of introducing our incremental modelling approach, we are going to sketch the fundamental material including modelling paradigms together with related semantics.

2.1 Hybrid Petri nets

Hybrid modelling and simulation of biological systems capture system dynamics that are characterised by a combination of deterministic and stochastic behaviours [7, 15]. Biological processes with fast reactions occur very often and thus are better be modelled deterministically, whereas biological processes with low number of species molecules and slow reactions occur infrequently and thus are better be modelled stochastically. To this end, $\mathcal{HPN}$ [16, 8, 9, 17, 18] comprise various modelling elements ranging from continuous places and continuous transitions to discrete places and stochastic transitions.

Continuous places hold real numbers as tokens representing species concentration. Continuous transitions represent reactions that occur continuously, i.e. continuous rates of changes in species concentrations. In addition to continuous modelling means, $\mathcal{HPN}$ support discrete place/stochastic transitions. A discrete place holds a discrete number of tokens to represent discrete states of a system, whereas a stochastic transition gets assigned stochastic firing rates determining a stochastic waiting time before the actual firing occurs. It is worth noting that a continuous/stochastic transition occurrence, i.e., transition firing, takes place only if the transition is enabled. In this context, an enabled transition is a transition whose pre-places hold a number of tokens greater than or equal to the number of tokens specified over the connecting arcs, i.e. arc weights. Firing a stochastic transition leads to removing a number of tokens from all pre-places and adding a number of tokens to all post-places, both according to the weights specified over the connecting arcs. Likewise, firing a continuous transition leads to a continuous decrease of the token values on all pre-places and an increase on all post-places.

Additionally, the following set of special transitions is supported by $\mathcal{HPN}$: immediate transitions, deterministically delayed transitions, and scheduled transitions [7, 19]. The firing of these transitions follows inherently different principles. Immediate transitions fire immediately as soon as the enabling condition holds. Deterministically delayed transitions fire after deterministic time delays, and the firing of scheduled transitions respects a pre-defined time schedule. These special transitions are specifically of help to represent discrete events of a system. In addition, $\mathcal{HPN}$ offer a set of special arcs including read, inhibitory, equal, and reset arcs. These modelling features are described in Table 1 with simple explanatory examples.

Table 1. $\mathcal{HPN}$ modelling features with explanatory examples.

Class	Element	Simple Example	Description
Transitions and Places	Continuous	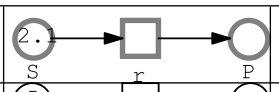	Reaction r occurs continuously over time, describing the rate of change of the species S and P.
	Stochastic	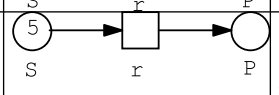	Reaction r occurs stochastically following Mass/action kinetic rate function.
	Deterministic	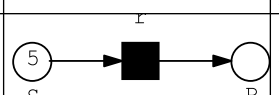	Reaction r occurs after time delay 20.
	Immediate	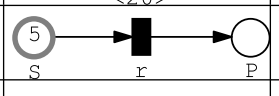	Reaction r occurs immediately (no time delay).
	Scheduled	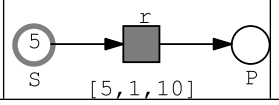	Reaction r occurs at the period starting from time point 5 till time point 10, i.e. 6 times.
Arcs	Read	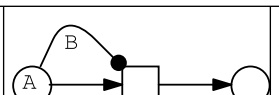	Reaction r occurs only when the condition $S \geq B$ hold.
	Inhibitor	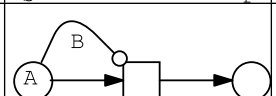	Reaction r occurs only when the condition $S < B$ hold.
	Equal	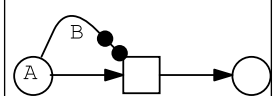	Reaction r occurs only when the condition $S == B$ hold.
	Modifier	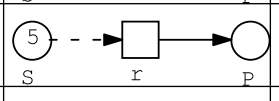	The reaction r occurs with rate S.
	Reset	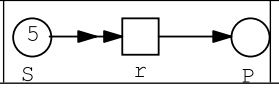	The place S will reset once reaction r occurs.

Hybrid Petri nets are formally defined by the following tuple $\mathcal{HPN} = \langle P, T, A, F, V, m_0 \rangle$ [15, 18], where :

- $P = P_{disc} \cup P_{cont}$ is the set of places, with P_{disc} is the set of discrete places and P_{cont} is the set of continuous places.
- $T = T_s \cup T_i \cup T_d \cup T_{sched} \cup T_{cont}$ is the set of transitions, with T_s is the set of stochastic transitions, T_i is the set of immediate transitions, T_d is the set of deterministically delayed transitions, T_{sched} is the set of scheduled transitions, and T_{cont} is the set of continuous transitions. $T^D = T_s \cup T_i \cup T_d \cup T_{sched}$ denotes the subset of discrete transitions.
- $P \cap T = \emptyset$.
- $A = A_{disc} \cup A_{cont} \cup A_I \cup A_T \cup A_E \cup A_R \cup A_M$ is the set of directed arcs with $A_{disc} \subseteq (P \times T^D) \cup (T^D \times P)$ defines the set of discrete arcs, $A_{cont} \subseteq (P_{cont} \times T_{cont}) \cup (T_{cont} \times P_{cont})$ defines the set of continuous arcs, $A_T \subseteq (P \times T)$ defines the set of read arcs, $A_I \subseteq (P \times T)$ defines the set of inhibitor arcs, $A_E \subseteq (P_{disc} \times T)$ defines the set of equal arcs, $A_R \subseteq (P \times T^D)$ defines the set of reset arcs, $A_M \subseteq (P \times T)$ defines the set of modifier arcs.

- F is a function

$$F : \begin{cases} A_{cont} \rightarrow, \mathbb{R}^+ \\ A_{disc} \rightarrow \mathbb{N}, \\ A_T \rightarrow \mathbb{R}^+, \\ A_I \rightarrow \mathbb{R}_0^+, \\ A_E \rightarrow \mathbb{N}, \\ A_R \rightarrow \{1\}, \\ A_M \rightarrow \{1\}. \end{cases}$$

  which assigns a positive integer value or a positive rational value as a weight to each arc depending on the arc type. If an arc is not explicitly weighted, we assume a weight of 1.
- V is a set of functions $V = \{g, w, d, f\}$ where :

  1. $g : T_s \rightarrow H_s$ is a function which assigns a stochastic hazard function h_{s_t} to each transition $t_j \in T_s$, that determines a random waiting time before transition firing.
  2. $w : T_i \rightarrow H_w$ is a function which assigns a weight function h_w to each immediate transition $t_j \in T_i$, such that $H_w = \{h_{w_t} | h_{w_t} : \mathbb{R}_0^{|{}^\bullet t_j|} \rightarrow \mathbb{R}_0^+, t_j \in T_i\}$ is the set of all weight functions, and $w(t_j) = h_{w_t}, \forall t_j \in T_i$.
  3. $d : T_d \cup T_{sched} \rightarrow \mathbb{R}_0^+$, is a function which assigns constant time to each deterministically delayed and three real values to each scheduled transition representing the beginning of the firing interval, the repetition value, and the end of the firing interval; respectively.
  4. $f : T_{cont} \rightarrow H_c$ is a function which assigns a rate function h_c to each continuous transition $t_j \in T_{cont}$.

- $m_0 = m_{cont} \cup m_{disc}$ is the initial marking for both the continuous and discrete places, whereby $m_{cont} \in \mathbb{R}^{+|P_{cont}|}_0$, $m_{disc} \in \mathbb{N}_0^{|P_{disc}|}$.

To execute an $\mathcal{HPN}$ model over time, both the continuous and stochastic parts have to be executed by respecting a synchronisation schedule governing the switching between them. The semantic behind the continuous part is described as a set of ODEs. Each continuous place is mapped onto one ODE equation describing the continuous change of the place value over time, see formula (1) [14]

$$\frac{dp_i}{dt} = \sum_{\forall t_j \in {}^\bullet p_i} F(t_j, p_i) \cdot f_j - \sum_{\forall t_j \in p_i^\bullet} F(p_i, t_j) \cdot f_j, \qquad (1)$$

where $F(t_j, p_i)$ is the arc connecting the transition t_j to the place p_i. Similarly, the notation $F(p_i, t_j)$ denotes the arc connecting the place p_i to the transition t_j. The notation f_j describes the firing rate of the transition t_j (see the formal definition). The notations ${}^\bullet p_i$, and $p_i^\bullet$ denote the pre- and post-transition(s) of the place p_i, respectively.

The stochastic part is simulated by generating different firing paths through the stochastic Petri net as approximating its continuous-time Markov chain (CTMC). Please note, constructing the CTMC could be infeasible as the state space could be very large. For this purpose, Gillespie's stochastic simulation algorithm [20, 21] is employed to determine when the next transition should fire and which transition to fire. Algorithm 1 gives a pseudo-code representation of the hybrid simulation as implemented in *Snoopy* [16].

Algorithm 1 Hybrid Simulation

Input: $\mathcal{HPN}$ model with initial state, simulation end time.
Output: Hybrid simulation traces over time.

```
construct the ODEs induced by the input model;
initialise output traces by model initial state;
while simulation end time is not reached do
    if there are no stochastic transitions then
        initilise the ODE solver with current marking;
        solve ODE system induced by Equation 1 until an event occurs;
        advance simulator clock by integrator time;
        update system state and output traces;
        if one or more immediate transitions are enabled then
            check immediate transitions;
        else if one or more deterministic transitions are enabled then
            check deterministic transitions;
        else
            check scheduled transitions;
        end if
    else
        //stochastic part
        calculate next time step (Gillespie time t);
        choose an enabled stochastic transition respecting Gillespie algorithm;
        fire the chosen transition and update system states;
        advance simulator clock by t;
    end if
    update the output trace by the current state;
end while
```

2.2 Fuzzy logic

Kinetic parameter uncertainty is a prevalent challenge accompanying modelling of biological processes. This uncertainty may be attributed to insufficient or imprecise experimental data during model construction [22, 23, 3].

Fuzzy logic is a powerful approach for capturing parametric uncertainty by allowing each uncertain kinetic parameter to be defined as a range of values and thus having a band of results reflecting the model behaviour against each value in the given range. In contrast to classical sets, whereby an element has a binary membership degree of 0 or 1, fuzzy logic introduces the concept of fuzzy sets [24]. A fuzzy set is a collection of elements where each element is assigned a membership degree represented by $\mu \in [0; 1]$. For example, Figure 1 (Sub-figure a) gives the definition of a species concentration, e.g *g1* being *high*.

In the crisp world, a species is categorized in this example as *high* if its concentration surpasses or equals 30 molecules —- signifying a membership degree of 1. Conversely, if the concentration falls below this threshold, it is designated as *low* with a membership degree of 0. In the context of fuzziness, the status of the species *g1* is *high* when its concentration falls within the range of $\pm$ 30 molecules. In our example, the membership degree varies from 0 to 1 within the range [20, 45], thereby characterising the gene concentration as uncertain. This uncertainty range is described by a fuzzy number as depicted in Figure 1 (Sub-figure b).

A fuzzy number is a special fuzzy set that is defined over a universal set $\mathbb{X}$. The commonly used fuzzy numbers are triangular fuzzy numbers (TFN for short). A triangular fuzzy number is defined by three points, i.e. $\tilde{\xi} = (a, b, c)$ with $a \leq b \leq c$. Figure 1 (Sub-figure b) presents a triangular fuzzy number representing the uncertainty range of a species concentration being high, where $a = 20$, $b = 30$ and $c = 60$. A possible interpretation behind these values per each point could be as follows: pessimistic value (a), the most possible value (b) and the optimistic value (c) of the concentration of the species *gene 1*. A triangular fuzzy number comprises a number of α-levels (also called α-cuts) consisting of a crisp

subset of $\mathbb{X}$, in which each element has a membership degree greater than or equal to the given level [24].

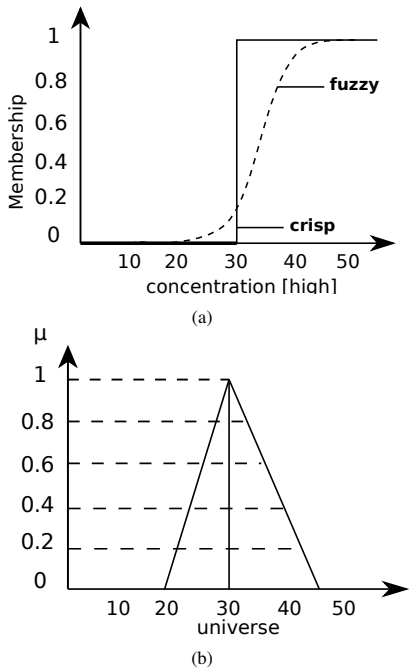

Fig. 1. (a) Two definitions of the set of a high concentration of the gene $g1$, a crisp set and a fuzzy set. (b) Triangular fuzzy number with six α-cuts describing the uncertainty range of the concentration of the gene $g1$.

In order to analyse kinetic parameter uncertainty, fuzzy (uncertainty) analysis techniques are employed [22, 3]. Performing uncertainty analysis for e.g. a biological system, whose input is uncertain (which is often the case for biological systems) results in a fuzzy band of each output variable. A fuzzy band reflects the uncertainty caused by each input over time. A distinct advantage that can be obtained from the fuzzy band is that the true trace that may lie in the band would be captured by matching experimental findings with those encompassing the fuzzy band, and thus capture the best match parameters which may fit with the modelled system.

Furthermore, performing uncertainty analysis gives membership functions over time for each output. Timed membership functions are helpful in capturing the uncertainty effect at a certain time point.

2.3 Fuzzy hybrid Petri nets

Fuzzy hybrid Petri nets extend hybrid Petri nets by allowing transition rates to involve uncertain kinetic parameters [3, 5]. $\mathcal{FHPN}$ give substantial expressive modelling power, as they combine stochastic and deterministic modelling means in one net class as well as permit to capture kinetic data uncertainty. In this context, each uncertain kinetic parameter is modelled as a TFN. Figure 2 sketches a diagram illustrating the modelling power of the $\mathcal{FHPN}$ as implemented in our powerful modelling and simulation tool *Snoopy* [16]. The diagram suggests that all the modelling elements that are given by Table 1 are offered by $\mathcal{FHPN}$ as well. It is worth noting that $\mathcal{FHPN}$ can be reduced to special fuzzy Petri net classes, namely fuzzy continuous Petri net ($\mathcal{FCPN}$) [25] by having merely continuous modelling means. Similarly, $\mathcal{FHPN}$ can also be reduced to another special fuzzy Petri net class, namely fuzzy stochastic Petri nets ($\mathcal{FSPN}$) [3].

The formal definition of fuzzy hybrid Petri nets is given as follows, with the symbol Γ representing the set of triangular fuzzy numbers including real numbers.

Fuzzy hybrid Petri nets are a 6-tuple $N = \langle P, T, A, F, v, m_0 \rangle$ where:

- $N = \langle P, T, A, F, v, m_0 \rangle$ is a hybrid Petri net.
- $v : T \rightarrow H$ is a function which assigns a firing rate function h_t to each transition $t \in T$, whereby $H = \{h_t | h_t : \Gamma^{|\bullet t|} \rightarrow \Gamma, t \in T\}$ which means that a kinetic parameter is described by either a fuzzy number or a real (crisp) number in Γ. Note that a combination of both crisp and fuzzy parameters is allowed. The assigned rate function is interpreted (depending on the transition's type) either in a stochastic or continuous manner.

To execute a fuzzy hybrid Petri net model, Zadeh's extension principle is adopted [26]. According to the extension principle, each fuzzy kinetic parameter is decomposed into its α-cuts. Then, each α-cut is discretised into a set of samples. If many fuzzy parameters are involved, then sample combinations of all fuzzy numbers are obtained. Afterwards, hybrid simulation is performed using each sample combination [11]. Consequently, each individual hybrid simulation will produce one trace of each variable (place). Thus, we can construct a band of traces of each variable over time. Each trace in the obtained band corresponds to one sample per α-cut. Therefore, we can also compose membership functions of each variable at each time point by obtaining minimum and maximum values. These steps are sketched by Algorithm 2 [5].

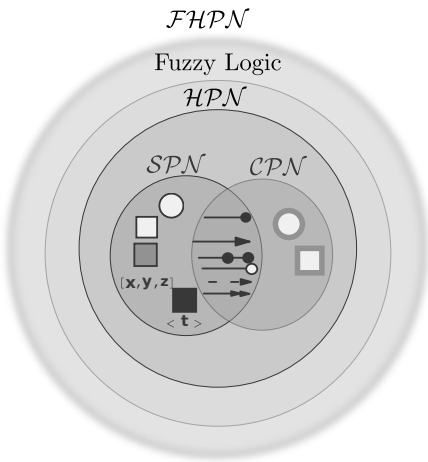

Fig. 2. A schematic diagram depicting the modelling power covered by $\mathcal{FHPN}$. The intersection between $\mathcal{SPN}$ and $\mathcal{CPN}$ reflects the shared modelling elements.

With $\mathcal{FHPN}$, we can offer a powerful but easy-to-use incremental modelling approach for biological systems, which usually works as follows. Each components is first reconstructed with distinct $\mathcal{FHPN}$ formalisms such as deterministic, stochastic, uncertain or hybrid ones, and then all the components are incrementally integrated together by defining meaningful interfaces with places and transitions of Petri nets. All these steps can be aided by Snoopy with friendly graphical user interface.

3 Results

3.1 A workflow for incremental modelling with $\mathcal{FHPN}$

The workflow sketched in Figure 3 starts off with modelling preparation. This step aims at gaining a sufficient understanding of the studied system for the sake of collecting the basic biological processes and associated activities characterising the system at hand. Next, an appropriate modelling paradigm including either deterministic, stochastic or hybrid variants has to be determined for constructing an $\mathcal{FHPN}$ basic model. At this

Algorithm 2 Fuzzy hybrid simulation.

Input: $\mathcal{FHPN}$ model with K fuzzy kinetic parameters, J number of alpha levels (α-cuts), number of samples per each level and sampling strategy.

Output: Fuzzy bands of all variables together with their membership functions over time.

for each α level α_j, j= 0, 1 , .. $J-1$ **do**
  for each fuzzy kinetic parameter k **do**
    compute α-cut set using j and k;
    perform sampling using the chosen sampling strategy;
  end for
  for each sample combination S of all fuzzy numbers **do**
    perform Algorithm 1;
  end for
end for
for each place p_i, i= 0, 1 , .. M **do**
  construct fuzzy band using all continuous simulation traces of p_i;
  compose membership functions of p_i at each time point;
end for

stage, an expert in Systems Biology may be of help for the purpose of determining the underlying semantics of the model. Afterwards, the basic model is simulated and validated against the experimental data. Then, we incrementally construct individual components. For the purpose of integrating the components into the basic component, we need to determine the component interfaces that will be used for integration. Gradually, the incremental model is simulated and validated for achieving the modelling goal.

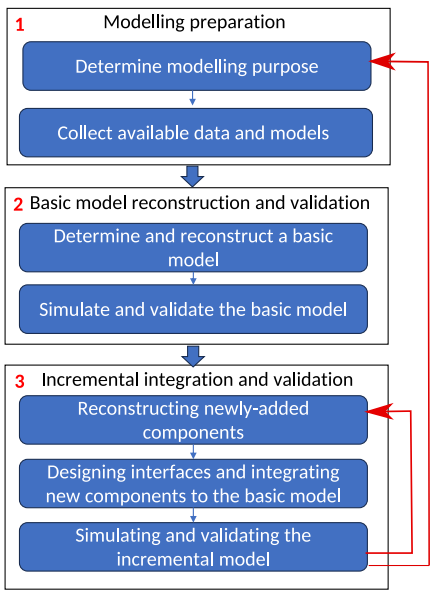

Fig. 3. A schematic diagram depicting the incremental modelling approach using $\mathcal{FHPN}$.

3.2 A case study

3.2.1 Modelling preparation

In the modelling preparation step, we first need to determine the modelling purpose of the biological system to be studied and then collect available data, e.g. experimental data and/or existing model components that could have been built by different organisations with different modelling formalisms. In this paper, we are going to demonstrate our approach with the cholesterol and lipoprotein metabolism and hypercholesterolemia therapy.

Dietary or external cholesterol only contributes to 20% of the body's total cholesterol. The remaining 80%, known as endogenous cholesterol, is primarily synthesized by hepatocytes [27]. Nevertheless, cells within the central nervous system and reproductive organs also play a role in cholesterol production. Each cell is subject to the cholesterol biosynthesis cascade initiated by the 3-Hydroxy-3-Methylglutaryl-Coenzyme-A Reductase (*HMGCR*) gene [27]. A cell controls the rate of cholesterol production (according to its needs) by means of a transcription factor, the sterol regulatory element-binding protein 2 (SREBP-2 or $S2$ for short) [28, 29]. The transcription factor $S2$ [30] is blocked from upregulating mRNA transcription of the *HMGCR* gene when cholesterol levels are high, but it is free to upregulate *mRNA* transcription when levels are low. Cholesterol and fats originating from a normal diet are transported through the bloodstream into cells by means of lipoproteins [31]. Lipoproteins end up in the liver which is responsible for removing them from circulation by a process known as receptor-mediated endocytosis (RME) [31].

There are five classes of lipoproteins [31, 32], among which, two classes have an essential role in cholesterol metabolism, namely low density lipoprotein (*LDL*) and very low density lipoproteins (*VLDL*). The former class carries a low amount of cholesterol, whereas the other one carries a high amount of cholesterol. The rate of lipoprotein uptake is regulated by the number of available *LDL* receptors (*LDLRs*) on the cell surface. *LDLRs* synthesis is governed by $S2$. When intracellular cholesterol levels are low, *LDLR* transcription is elevated, leading to a greater uptake of lipoproteins. In the same way, high levels of cholesterol lead to the downregulation of *LDLR* concentration, which means decreasing lipoprotein endocytosis [33]. Two courses of therapy have been used to treat elevated levels of cholesterol (hyperlipidemia). First, statin is a group of drugs that act to reduce levels of fats including triglycerides and cholesterol in the blood [34]. Second, proprotein convertase subtilisin kexin type 9 (PCSK9) is a specific regulatory protein blocking the cell uptake of LDL-cholesterol from plasma by directly interacting with *LDL* receptors, and thus it leads to the degradation of the *LDL* receptors [35].

Figure 4 presents a diagram illustrating the biological activities of cholesterol regulation inside a liver cell (hepatocytes). These activities occur in three areas of the liver cell. First, the genetic regulation of *HMGCR* and *LDL* receptors occurs in the cell nucleus compartment. Second, all processes related to *VLDL* and *LDL* binding and breakdown, cell receptor and cholesterol regulation occur in the cell cytoplasm compartment. Please note that the cytoplasm is surrounded by the cell membrane. Finally, *VLDL* and *LDL* sources and *VLDL* to *LDL* delipidation occur in the extracellular space.

In this case study, we are going to study hypercholesterolemia therapy from two aspects: dosing the statin drug over time, and dosing the PCSK9 antibodies at the beginning of the simulation, for which we will construct two incremental models in order to show the flexibility and convenience of our approach. Correspondingly, we collect three components: basic cholesterol and lipoprotein metabolism, statins therapy, and PCSK9 therapy.

3.2.2 Basic model reconstruction and validation

The second step is to reconstruct basic models with $\mathcal{FHPN}$ or even to construct basic $\mathcal{FHPN}$ model components directly from experimental data. This step could be further divided into several sub-steps, which are given as follows.

***D**etermine and reconstruct a basic model.* We first need to determine a basic model from which an incremental model can be started and then reconstruct the model with $\mathcal{FHPN}$. In this case study, we start from the

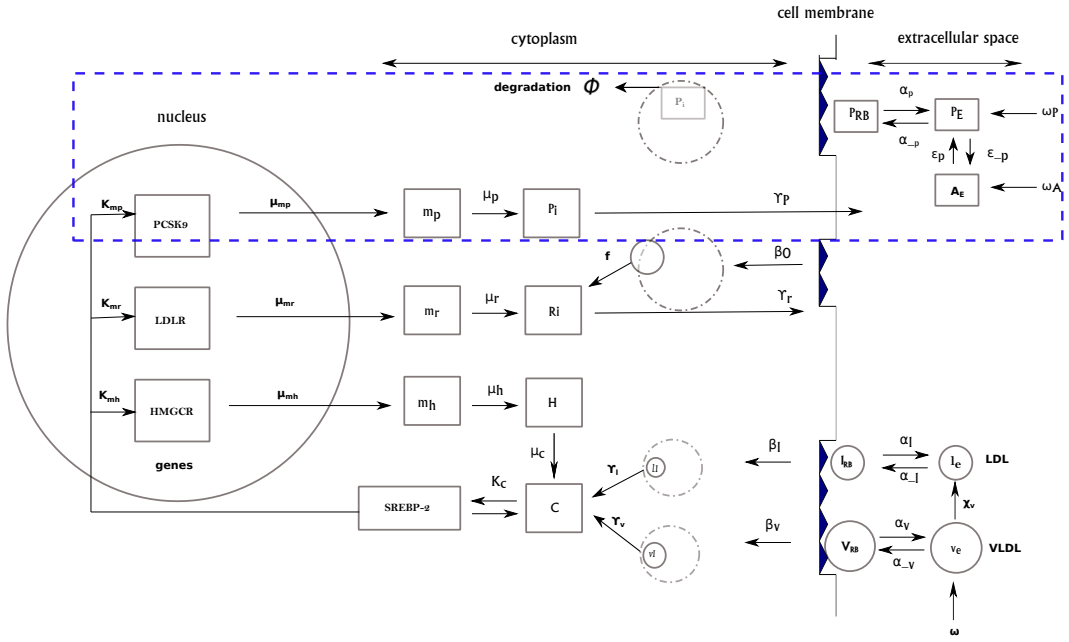

Fig. 4. A schematic diagram depicting the cholesterol and lipoprotein metabolism (in a hepatocyte) and the hyperlipidemia therapy. The area surrounded by the blue-dashed box represents the therapy using the PCSK9 as given in [35]. The S_2 protein (with rates K_{mh}, K_{mr} and K_{mp}) stimulates the transcription and the synthesis of HMGCR (H), low-density lipoprotein receptor (R), and PCSK9 (P) mRNA in the cell nucleus and cytoplasm. The transcription of the genes occurs at rates μ_{mh}, μ_{mr} and μ_{mp}, while the synthesis of mRNAs occurs at rates μ_h, μ_r and μ_p. Cholesterol production occurs by negatively regulating SREBP-2 (K_c) and the activity of HMGCR (μ_c) [29]. The LDLR (R_i with rate constant γ_r) and PCSK9 (P_i with rate constant γ_p) are transported to the cell membrane and extracellular space. In the extracellular space, lipids are removed from VLDL, i.e. VLDL delipidates to LDL (with rate constant X_v), and each bind/unbind to LDLR (l_{RB} and V_{RB}) on the cell surface with rates α_v, α_{-v}, α_l and α_{-l}. w is a constant supply of VLDL to the serum. Then, LDLRs are transported into the cell cytoplasm with rates β_l and β_v. Consequently, cholesterol (C) is extracted from lipoproteins (at rates γ_v andγ_l). Interaction of PCSK9 with anti PCSK9 agents (A, ε_p) also occurs in the extracellular space. It is worth noting that the constants ω_p and ω_A represent temporary sources of external PCSK9 and anti-PCSK9 agents, respectively.

basic cholesterol and lipoprotein metabolism model. The basic cholesterol and lipoprotein metabolism is identified as a deterministic process [33, 35], and thus this process is described as a set of ODEs representing the biochemical activities that are sketched in Figure 4. Therefore, we model this process as a deterministic component using the continuous modelling elements of $\mathcal{FHPN}$. Figure 5 gives an $\mathcal{FHPN}$ model of the cholesterol and lipoproteins metabolism, which exactly describes the mathematical model given in [33]. The presented model comprises the activities at the genetic level including the *HMGCR* transcription by the $S2$ gene (represented as a rate constant). The yellow part represents the transcription of the *HMGCR* gene (m_h), which leads to the synthesis of the *HMGCR* (h). The blue part represents the transcription of *LDLR mRNA* which leads to the synthesis of *LDLR* (receptor). The red part models cholesterol synthesis (c) and its degradation. The transitions $sync1\_c$ and $sync2\_c$ contribute to the synthesis of cholesterol by extracting it from the internalised lipoproteins (*LDL* and *VLDL*) which are highlighted in orange colour, whereas the transition $sync3\_c$ encodes cholesterol production inside a liver cell which is stimulated by the *HMGCR* activity. Note that each synthesis activity is followed by a degradation activity (the transitions starting with the prefix deg). It is worth noting that this model is equivalent to a $\mathcal{CPN}$ model as there are no discrete places or discrete transitions (which also precludes stochastic transitions) nor fuzzy kinetic parameters involved. To become familiar with the description of the model places as well as the underlying ODE equations, please consult the supplementary material $S1$.

***S**imulate and validate the basic model.* Next, we can simulate our reconstructed model and then validate it against the original model or experimental data. Figure 6 presents numerical simulation results of the $\mathcal{FHPN}$ model given in Figure 5. This model has been deterministically interpreted, as there is no discrete part. Note also that the $\mathcal{FHPN}$ model is automatically turned into a non-fuzzy model as there are no fuzzy kinetic parameters involved. Initially, the *HMGCR mRNA* (m_h) and $LDLR$ receptor mRNA (mr) concentrations increase in response to zero cholesterol (c) in the system, which leads to an increase in *HMGCR* concentration (h). The internal cholesterol level is increased by the extracted cholesterol from lipoproteins. Consequently, the concentration of *HMGCR* and *LDLR mRNA* decreases. This is reflected by the oscillatory behaviour in the system. After that, the system approaches a steady condition. For traces showing the evolution of other places representing, e.g. *LDL/VLDL* lipoproteins, please consult the supplementary material of this paper $S1$.

3.2.3 Incremental integration and validation

Assume we already have reusable components available, then we can start the incremental integration and validation of these components, which can be further divided into three main sub-steps: reconstructing newly-added components, designing interfaces and integrating new components to the basic model, and simulating and validating the incremental model. Among these steps, how to design the correct interfaces of two components is most important. In the following, we will show how to implement two incremental models.

(1) **Modelling statin drugs therapy**

***R**econstructing newly-added components.* We extend the basic model of cholesterol and lipoproteins metabolism presented in Figure 5 by a statins therapy modelling component. Statins are a common pharmaceutical treatment for reducing elevated levels of plasma cholesterol. These drugs bind to *HMGCR* preventing the binding with the 3-hydroxy-3-methylglutaryl coenzyme-A (HMGCoA coenzyme), and thus inhibiting cholesterol biosynthesis [33, 35]. According to *Pool et al.* [33], modelling

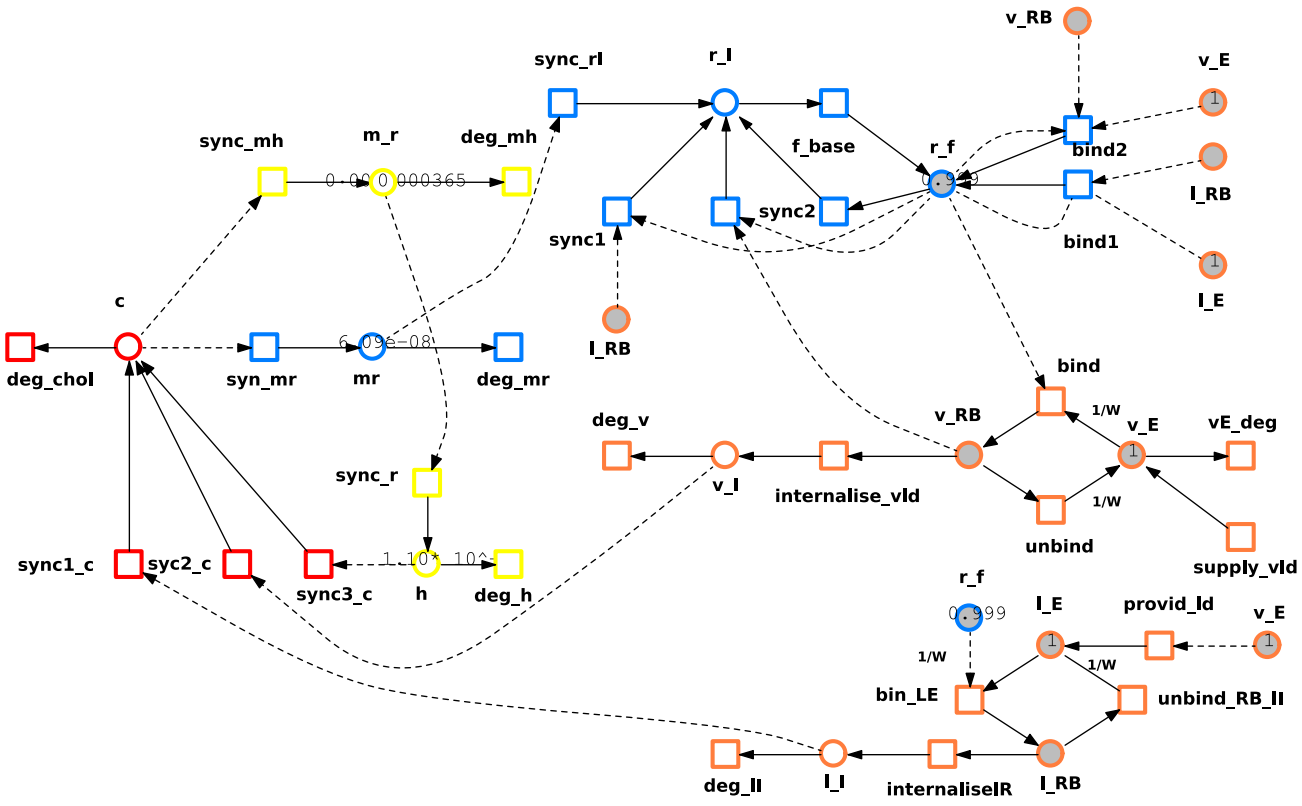

Fig. 5. $\mathcal{FHPN}$ of cholesterol and lipoprotein metabolism, corresponding to the explanatory diagram depicted in Figure 4. Note that the PCSK9 therapy is not considered in this model. The transitions syn_mh, $sync\_mr$ and syn_h describe the transcription, translation and synthesis activities (inside the cell nucleus) of HMGCR (h) and LDLR (mr), respectively. These activities are activated by SREBP-2 protein (modelled as a rate constant). The degradation of each product is modelled as a post-transition. Afterwards, HMGCR (h) is used to produce cholesterol inside the cell. The right-hand subnet (orange) represents how cholesterol (place c) is extracted from the internalised lipoproteins (whose binding/unbinding occurs in the external space of the cell modelled as a reversible reaction); here the extracted cholesterol contributes to cholesterol production in the liver cell (transitions $syn1\_c$ and $syn2\_c$). Dashed arcs are called modifier arcs permitting the connected place to occur as a constant of the target transition. It is worth noting that some places of the model are logical places (marked by the gray colour). These places having identical names refer to the same place to improve model readability.

statins therapy can be achieved by modifying the transcription of *HMGCR mRNA* (μ_{mh}), which leads to the down-regulation of the intracellular cholesterol concentration and up-regulation of the receptor synthesis and thus increasing the amount of lipoproteins degraded. In this paper, we model doses of statins drugs according to the following formula:

$$\mu_{mh} = \begin{cases} 0, 10 \text{ min} + n \cdot 14 \text{ h } 45 \text{ min} \leq t \leq 23 \text{ h} + n \cdot 14\text{h } 45 \text{ min}, \\ 1.406{\cdot}10^{-7}, \text{otherwise} \end{cases}$$

where n is the number of dosage periods. Let us consider two doses of the statin drug, i.e. $n = 2$. This means that the dosage will be applied in the course of the following two periods: from approx. 10 to 23 and from 24 to 38 (hour). This dosage schedule is modelled by disabling the pre-transition of the place m_h (by multiplying the rate function with zero) during the given dosage period; otherwise, we multiply the rate function with one. Please note that the value of the transcription factor μ_{mh} is equal to $1.406{\cdot}10^{-7}$ during simulation. By means of the $\mathcal{FHPN}$ modelling elements, this logic is modelled by using a flag (the place *statins_supply*) enabling/disabling the statins dosage. Each dosage period is modelled by connecting a scheduled transition to the flag using a reset arc. This leads to resetting the flag as soon as the scheduled transition gets fired. In order to set the flag (with the value 1) we connect the flag place with an immediate transition which is assumed to be enabled in the non-dosage periods (using another scheduled transition). After the two doses were applied, we set the flag again by making use of a deterministic transition which fires when time 38 h is reached; see the $\mathcal{HPN}$ model presented in Figure 7. Please note, for the purpose of our modelling objectives, stochastic transitions are neither required nor useful to describe the statins therapy component.

***D**esigning interfaces and integrating new components to the basic model.* After designing model components, basic cholesterol metabolism components as well as dosage schedule component. Model integration is achieved by choosing place/transition interfaces connecting both components together. On one hand, the transition $sync\_mh$ is chosen as an interface (from the cholesterol metabolism component), as it is the starting point of modelling the drug dosage. On the other hand, the place $statins\_supply$ (from the schedule component) is chosen as interface place to the other component, as it enables/disables the drug dosage.

***S**imulating and validating the incremental model.* In the following, we provide hybrid simulation traces of the model describing the statins therapy. Figure 8 gives the traces of the inserted component describing the statins supplement. These traces show how cholesterol concentration rapidly declines upon supplying statins drugs at time points 9.75 and 24. Initially, the flag (place *statins_supply*) is set leading to the increase in cholesterol concentration. When the time point 9.75 is reached, the scheduled transition *reset_mh_1* will fire until the time point 23 is reached. During this firing period, the flag place will be reset (empty place) leading to the inhibiting of the *HMGCR mRNA* transcription and thus declining the cholesterol concentration.

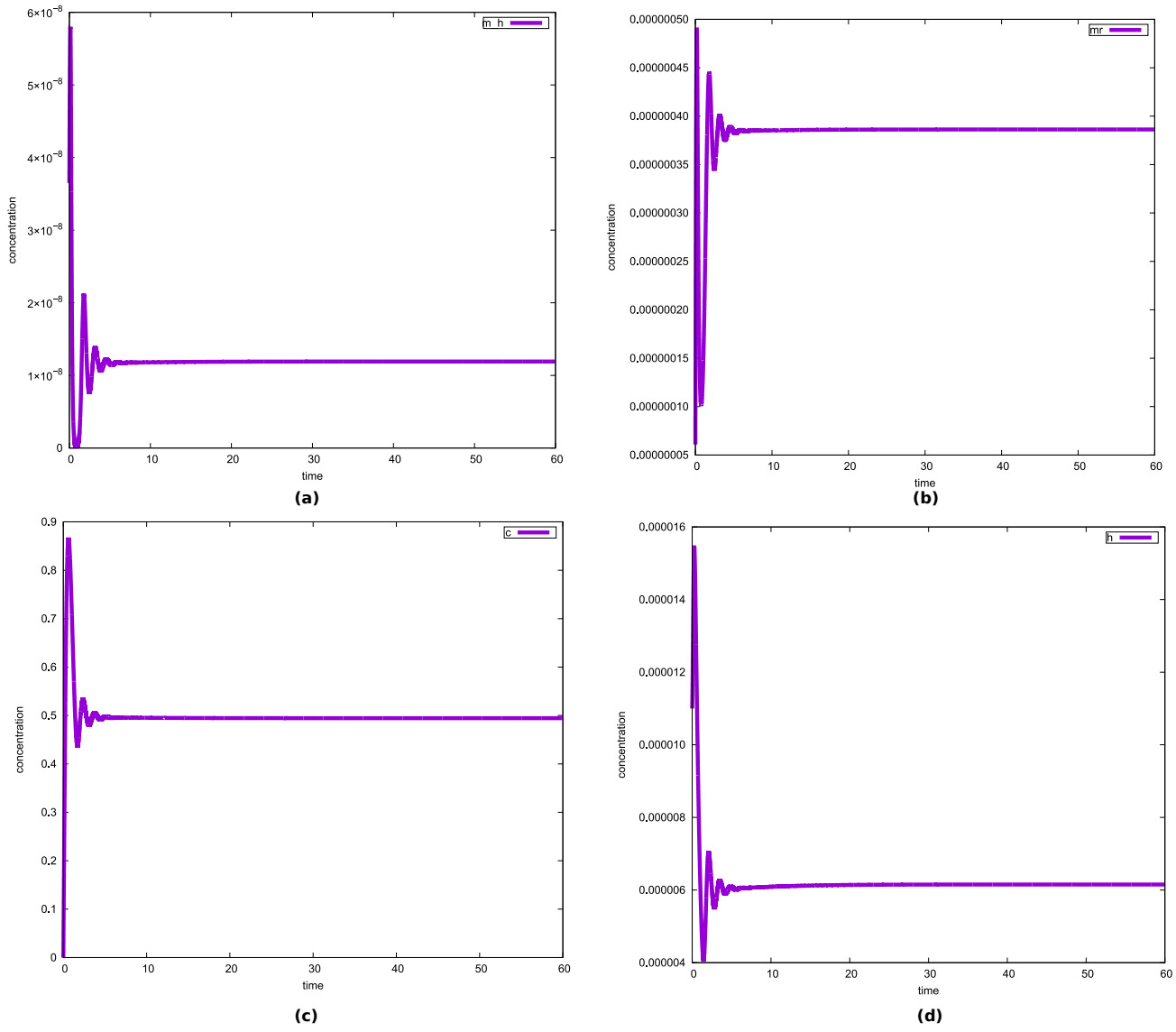

Fig. 6. Simulation traces of the cholesterol and lipoproteins metabolism. (a) HMGCR mRAN (place m_h). (b) LDL receptor mRNA (place mr). (c) Cholesterol concentration (place c). (d) HMGCR concentration (place h).

Figure 9 provides simulation traces of the hybrid model. These traces show that upon receiving a statin dose, the concentrations of *HMGCR mRNA* (place m_h) dramatically drop to zero, as the transcription activity is inhibited. Consequently, cholesterol levels decline significantly which in turn up-regulates the transcription of receptor mRNA (place mr) as a response by the cell to provide more cholesterol to maintain healthy levels. Our analysis results are in line with the study conducted by *Pool et al.* in [33]. For other traces of the model variables, please check the supplementary material.

(2) **Modelling PCSK9 therapy.**

***R**econstructing newly-added components.* We construct an incremental model describing the therapy of elevated levels of cholesterol. We add two components to the basic cholesterol metabolism model to describe both the PCSK9 therapy and uncertainty of kinetic parameters. Figure 10 presents a fuzzy hybrid Petri net incorporating the anti-PCSK9 antibodies therapy into the basic model sketched in Figure 4. Please note that we use deterministically interpreted $\mathcal{FHPN}$, as we apply anti-PCSK9 antibodies at zero time point. This means that there is no need to handle discrete events while performing numerical simulation; thus this model can be seen as an $\mathcal{FCPN}$ model.

In the literature [33, 35], sensitivity analysis has been conducted in order to estimate the nominal values of model parameters. Sensitivity analysis gives a measure of how much variations in an input variable affect the results for a mathematical model. We offer here an uncertainty analysis approach with fuzzy continuous Petri nets to explore kinetic parameter uncertainty.

In order to illustrate our approach, we choose the following kinetic parameters to get assigned as fuzzy kinetic parameters (represented as triangular fuzzy numbers): the transcription factor SREBP (k_c), and the parameters of PCSK9-receptor binding/unbinding (α_p and α__p). These parameters have been chosen to get assigned uncertain values as the sensitivity analysis performed by [35] suggests that the values of these parameters have an impact above 50% relative to the steady-state values on the model variables. This suggests that their *nominal* values are worth

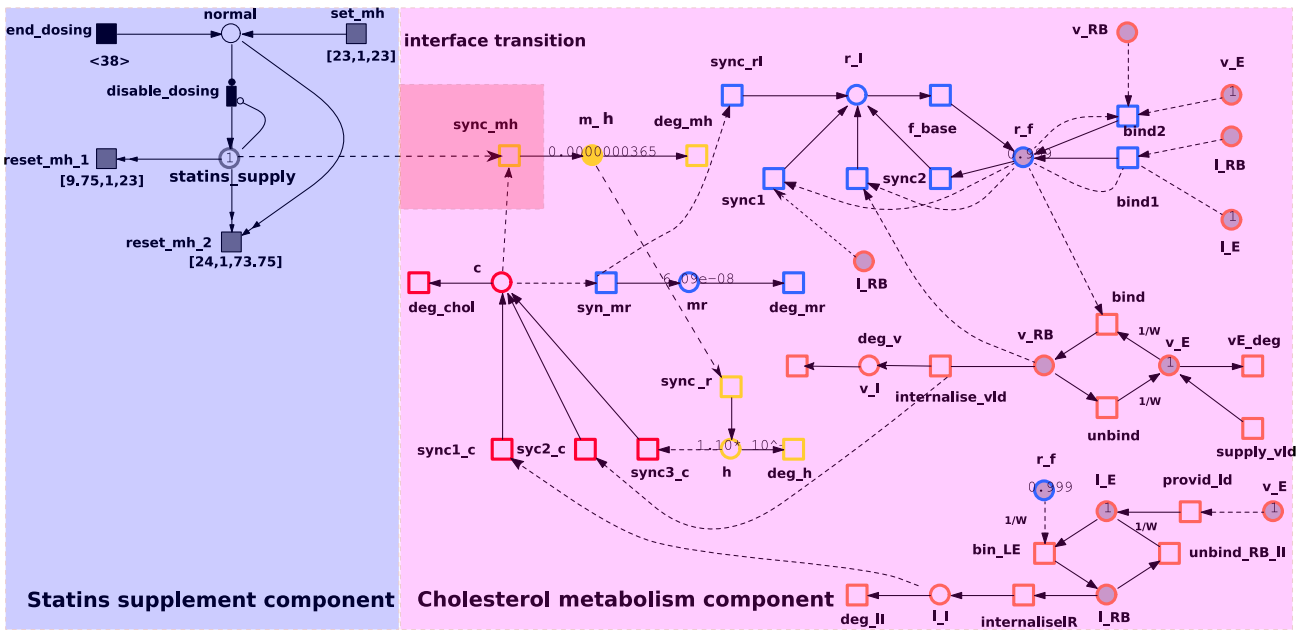

Fig. 7. $\mathcal{FHPN}$ of the cholesterol and lipoproteins metabolism with statins therapy. The net comprises two components connected by the interface transition $sync\_mh$. Two doses of the statins drugs over two periods are modelled. The place statins_supply represents a flag for controlling the statins dosage course. The scheduled transition reset_mh1 resets the flag statins_supply between 9.75 (h) and 23 (h), which means inhibiting HMGCR transcription. In order to activate the transcription between 23 (h) and 24 (h), we add the scheduled transition set_mh which will trigger setting the flag statins_supply by adding a token to the place normal and then the immediate transition disable_dosage will fire causing the flag to be set and thus getting back to the normal behaviour. The scheduled transition $reset\_mh\_2$ models the next dosage period. After time 37.75 (h), the flag will always be zero, so to switch to the normal behaviour, we use a deterministic transition which will fire after time point 38, causing the discrete place normal to have a token and thus the immediate transition to fire which in turn sets the flag again.

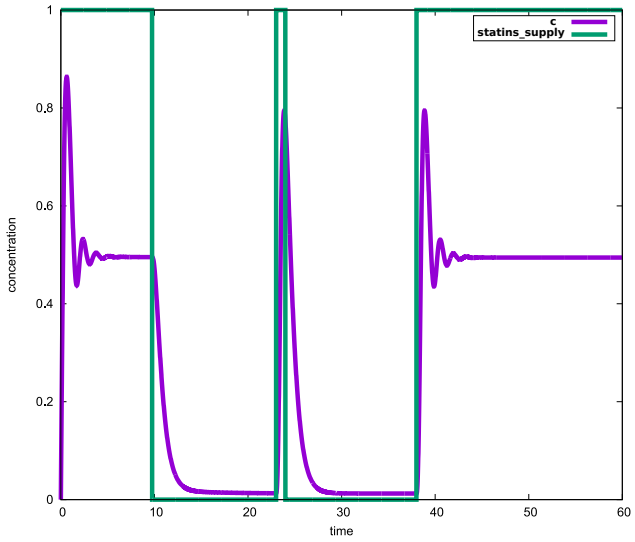

Fig. 8. Hybrid simulation traces of cholesterol (place c) versus statins supply flag (place statins_supply).

being scrutinised in more detail. In this way we will be able to explore how the variability of these input parameters would affect *LDL, VLDL*, and cholesterol concentration due to the therapy using anti-PCSK9 antibodies.

***D**esigning interfaces and integrating new components to the basic model.* For the purpose of integrating the anti-PCSK9 component (whose modelling elements are marked with green in Figure 10) into the cholesterol metabolism component, we have to select two interface places and one interface transition as shown in Figure 10, these interface places/transitions control both concentrations of PCSK9 mRNA and unbound receptor of lipoproteins [35]. The fuzzy component is represented by uncertain kinetic parameters that are assigned to the model.

***S**imulating and validating the incremental model.* Performing Algorithm 2 gives the fuzzy bands of the *LDL* cholesterol concentration (place c), shown in Figure 11. The anti-PCSK9 antibodies decrease the internalised *LDL* and *VLDL* levels (we confine ourselves to show only the LDL trace), and thus decrease cholesterol in the liver cell. Comparing the upper bounds of the internalised *LDL* and cholesterol with the traces presented for our plain model (no therapy courses), we notice low levels of both *LDL* and cholesterol, confirming the results given in [35].

To derive more precise knowledge about the upper and lower bounds of the concentrations over time as well as to capture the model's variability according to our analysis, we construct the fence plot sketched in Figure 11 (Sub-figure b) reflecting how upper and lower bounds of cholesterol change over simulation time.

For reproducibility purposes, the models presented in this paper can be accessed via `https://www-dssz.informatik.tu-cottbus.de/DSSZ/Software/Examples` together with the *supplementary material describing the models of the presented biological case study*. *Snoopy* is also available at `https://www-dssz.informatik.tu-cottbus.de/DSSZ/Software/Snoopy`.

4 Discussion

We summarise the main experience and lessons learnt while developing the presented case study for demonstrating the incremental modelling approach using $\mathcal{FHPN}$.

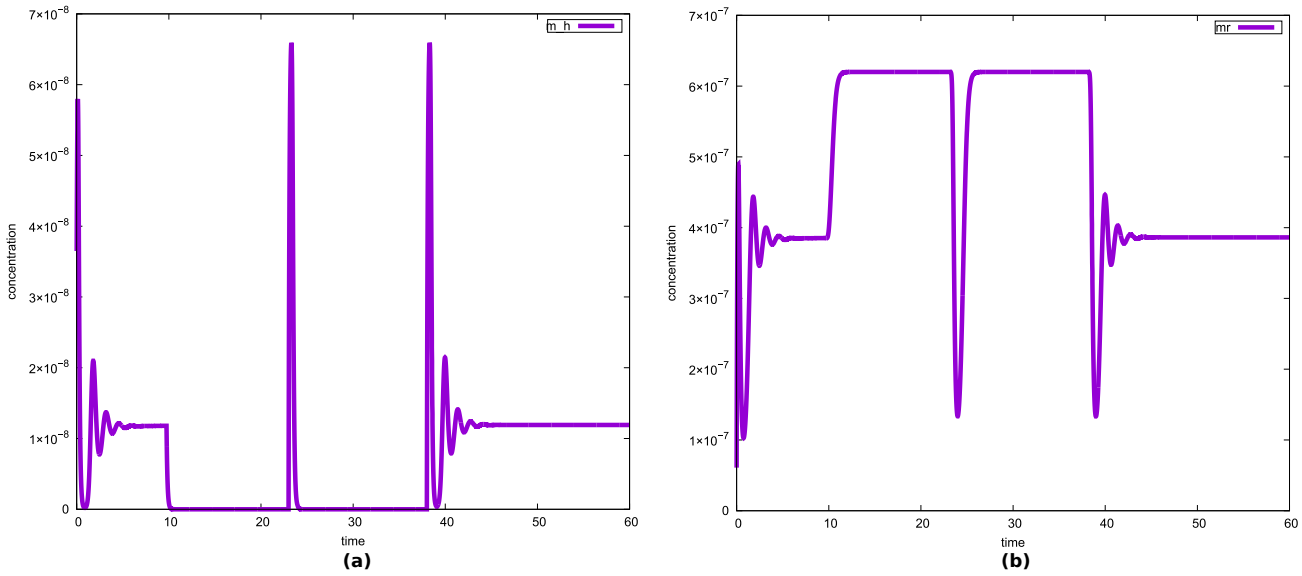

Fig. 9. Hybrid simulation of the cholesterol and lipoproteins model with the statins therapy. HMGCR mRNA concentration versus LDLR mRNA concentration within statins dosage schedule.

$\mathcal{FHPN}$ offer a powerful tool for incremental modelling of biological systems with multiple complementary modelling paradigms. In this context, continuous modelling elements are a modelling paradigm equivalent to ordinary differential equations. However, $\mathcal{FHPN}$ outperform traditional ODEs by their graphical and elegant modelling style. Furthermore, the discrete modelling elements of $\mathcal{FHPN}$ such as discrete places, discrete transitions, and special arcs are outstanding graphical means to represent various biological aspects. Moreover, fuzzy modelling is an excellent tool for exploring kinetic data uncertainty that can occur in both deterministic and/or discrete parts of a model. With $\mathcal{FHPN}$, each component can be separately modelled using a suitable paradigm and then validated against available experimental data or experts. After that, they can be incrementally integrated by developing meaningful interfaces for interacting two components by place or transition elements of Petri nets. This simple component-interface mechanism greatly facilitates the incremental modelling of biological systems. By resorting to incremental modelling techniques offered by $\mathcal{FHPN}$, we are gradually gaining more insights into the mechanism of a biological system.

A model/component repository can be easily constructed for specific biological systems with the help of $\mathcal{FHPN}$, which promotes the accumulation of knowledge about biological systems to be studied. As more models and components are added to the repository, researchers can better understand and analyse the intrinsic behaviour of these systems. For instance, for the cholesterol metabolism, we constructed different components, each representing a different aspect that could be utilised for further exploring the case study. This can lead finally to deeper insights and discoveries in the field of systems biology.

$\mathcal{FHPN}$ could be further extended using data-driven machine learning methods. Clarifying the mechanisms of biological systems is the primary goal of systems biologists. However, this task is exceptionally challenging due to the complexity of biological organisms and the limitations of current experimental and analytical tools. With the advancements in machine learning techniques, we will be able to construct more easily black-box data-driven models or model components that focus on the behaviour rather than the underlying mechanisms of biological systems. Integrating FHPN with data-driven methods will enable us to build much larger models, providing deeper insights into the functioning of the biological systems under study.

List of abbreviations

CPN: continuous Petri nets
CTMC: continuous-time Markov chain
FCPN: fuzzy continuous Petri nets
FHPN: fuzzy hybrid functional Petri nets
FSPN: fuzzy stochastic Petri nets
LDL: low-density lipoprotein
ODEs: ordinary differential equations
PCSK9: proprotein convertase subtilisin kexin type 9
PN: Petri nets
SSA: stochastic simulation algorithm
SPN: stochastic Petri nets
VLDL: very low-density lipoprotein

Funding

George Assaf was funded by *Katholische Akademische Ausländer-Dienst KAAD* scholarship. This work has been supported by National Natural Science Foundation of China (62273153).

A biographical note

George Assaf is a researcher with a doctorate degree in Computer Science, Brandenburg University of Technology Cottbus-Senftenberg. His research interests include modelling and simulating biological systems using quantitative (coloured) Petri nets covering stochastic, continuous and hybrid ones.

Fei Liu is a Professor in the School of Software Engineering, South China University of Technology. His research interests are modelling and simulation, Petri nets, and systems biology.

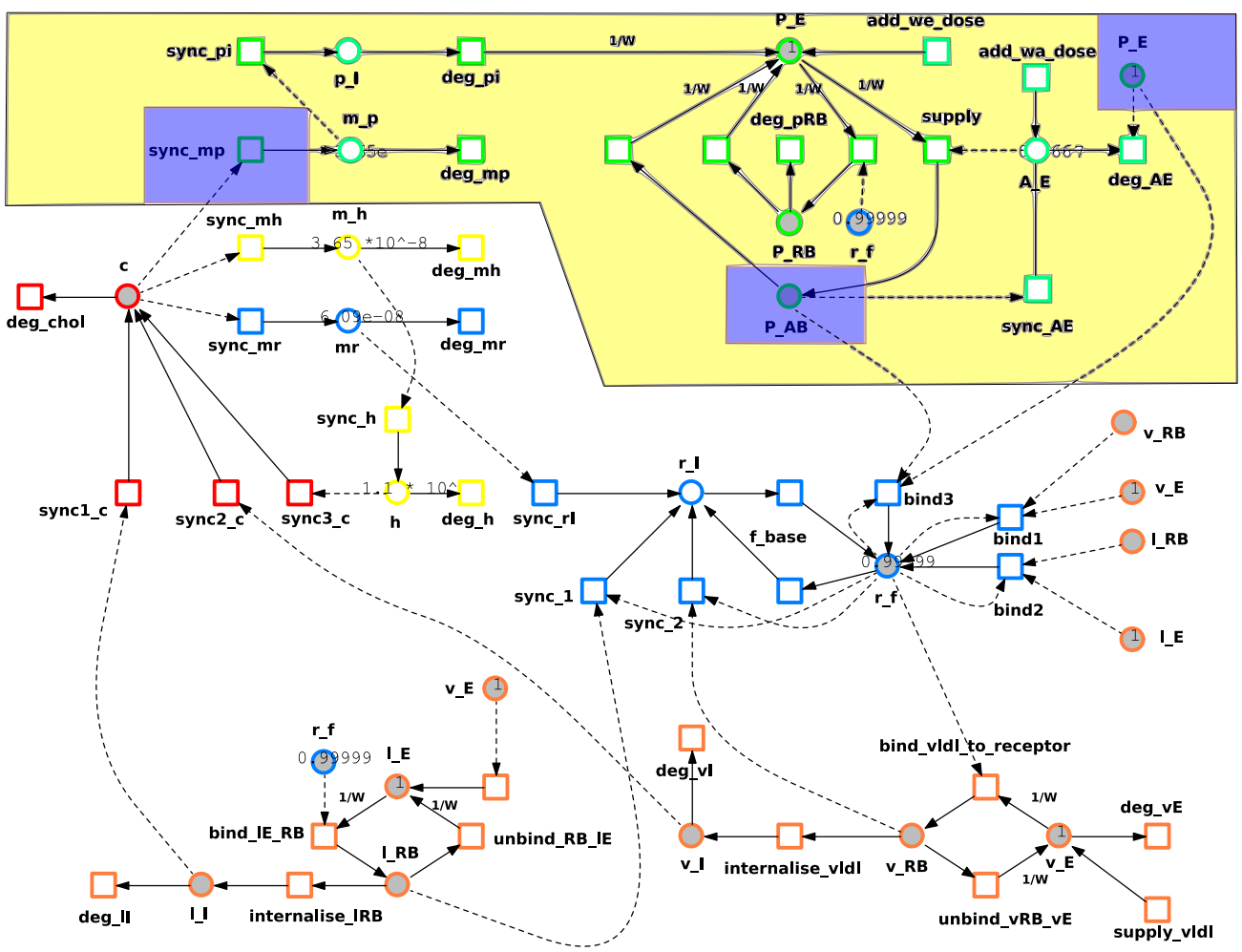

Fig. 10. Fuzzy hybrid Petri net model of the cholesterol and lipoprotein metabolism considering the therapy of elevated levels of cholesterol using anti-PCSK9 antibodies. The basic model of the cholesterol metabolism is extended by a new component describing the anti-PCSK9 antibodies therapy. The two components are connected by interface net elements that are surrounded by boxes. The green net elements represent the anti-PCSK9 extension. The place P_I holds the internalised PCSK9 concentrations. The places P_E and P_RB describe the unbound extracellular PCSK9 concentration and PCSK9 receptor-bound concentration. The place A_E holds unbound extracellular anti-PCSk9 agent concentration and the place P_AB holds the anti-PCSk9 agent bound concentration. Dosing anti-PCSK9 antibodies is expressed by the transition add_wa_dose; compare Figure 4 for more details on the relevant biological activities. The fuzzy kinetic parameters kc (cholesterol-SREBP-2 dissociation constant), alf_p (rate of PCSK9-receptor binding) and $alf\_\_p$ (rate of PCSK9-receptor unbinding) are assigned to the transitions $sync\_mh$, $bind3$ and $bind4$, respectively.

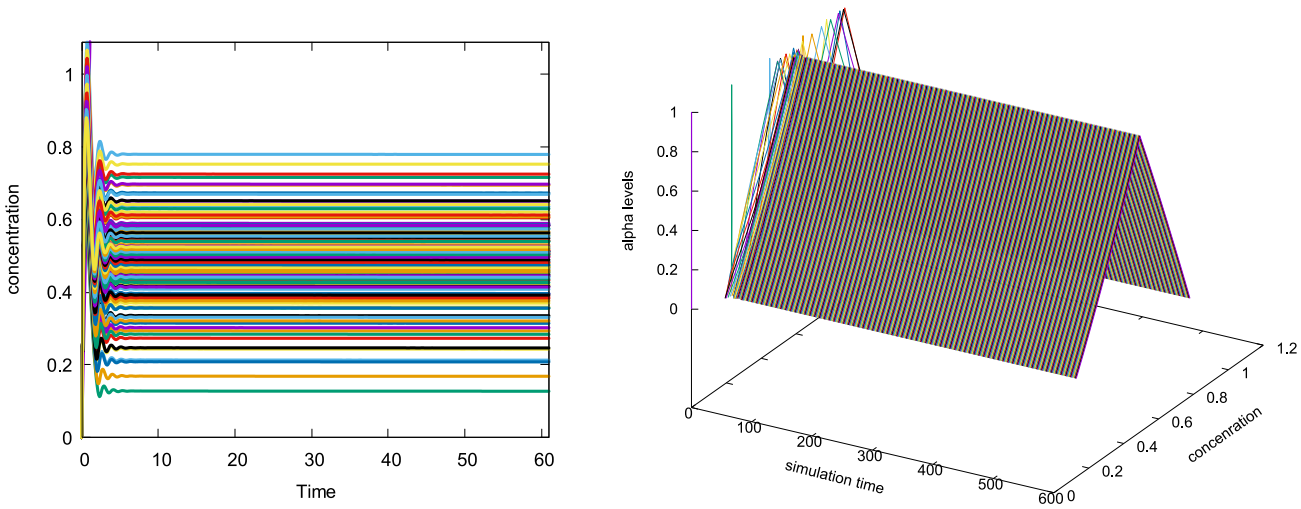

Fig. 11. (a) Fuzzy band of cholesterol (place c). (b) Fence plot of the timed-membership functions of the cholesterol concentration (place c).

Monika Heiner is a Professor (ret.) in the Department of Computer Science, Brandenburg University of Technology Cottbus-Senftenberg. Her research interests include modelling and analysis of technical as well as biochemical networks using qualitative and quantitative Petri nets, model checking, and simulation techniques.

Key points

- $\mathcal{FHPN}$ are a powerful tool for incrementally modelling biological systems with stochastic and/or continuous processes hampered by uncertain kinetic parameters.
- This paper sketches an incremental modelling workflow for aiding biologists to construct biological systems in a stepwise and intuitive manner.
- The presented workflow for modelling and analysis is applied to cholesterol and lipoprotein metabolism as a case study.

References

[1]R. David and H. Alla. *Discrete, Continuous, and Hybrid Petri Nets*. Springer, 2010.

[2]MA Blätke, M Heiner, and W Marwan. *BioModel Engineering with Petri Nets*, chapter 7, pages 141–193. Elsevier Inc., March 2015.

[3]G Assaf, M Heiner, and F Liu. Biochemical reaction networks with fuzzy kinetic parameters in Snoopy. In L Bortolussi and G Sanguinetti, editors, *Proc. CMSB 2019*, volume 11773 of *LNCS/LNBI*, pages 302–307. Springer, September 2019.

[4]The MathWorks Inc. Matlab version: 9.13.0 (r2022b), 2022.

[5]George Assaf. *Fuzzy coloured Petri nets for modelling biological systems with uncertain kinetic parameters* . PhD thesis, BTU Cottbus, Dep. of CS, December 2022.

[6]Wolfgang Reisig. Petri nets and algebraic specifications. *Theoretical Computer Science*, 80(1):1–34, 1991.

[7]M Heiner M Herajy. Hybrid representation and simulation of stiff biochemical networks. *J. Nonlinear Analysis: Hybrid Systems*, 6(4):942–959, November 2012.

[8]M Herajy, M Schwarick, and M Heiner. *Hybrid Petri Nets for Modelling the Eukaryotic Cell Cycle*, chapter ToPNoC, pages 123–141. Springer Berlin Heidelberg, 2013.

[9]M Herajy and M Heiner. Modeling and simulation of multi-scale environmental systems with generalized hybrid Petri nets. *Frontiers in Environmental Science*, 3(53), 2015.

[10]G Assaf, M Heiner, and F Liu. Coloured fuzzy Petri nets for modelling and analysing membrane systems. *Biosystems*, page 104592, 2022.

[11]G Assaf, M Heiner, and F Liu. Colouring fuzziness for systems biology. *Theoretical Computer Science*, 2021.

[12]C. ROHR. *Simulative analysis of coloured extended stochastic Petri nets*. PhD thesis, BTU Cottbus, Computer Science Institute, January 2017.

[13]R. David and H. Alla. *Discrete, Continuous, and Hybrid Petri Nets*. Springer, 2008.

[14]M Herajy and M Heiner. Adaptive and bio-semantics of continuous Petri nets: Choosing the appropriate interpretation. *Fundamenta Informaticae*, 160(1-2):53–80, 2018.

[15]Mostafa Herajy. *Computational Steering of Multi-Scale Biochemical Networks*. PhD thesis, BTU Cottbus, Dep. of CS, January 2013.

[16]M. Heiner, M. Herajy, F. Liu, C. Rohr, and M. Schwarick. Snoopy – a unifying Petri net tool. In *Proc. PETRI NETS 2012*, volume 7347 of *LNCS*, pages 398–407. Springer, 2012.

[17]M Herajy and M Heiner. Accelerated simulation of hybrid biological models with quasi-disjoint deterministic and stochastic subnets. In Eugenio Cinquemani and Alexandre Donzé, editors, *Hybrid Systems Biology: 5th International Workshop, HSB 2016*, LNBI, pages 20–38. Springer, 2016.

[18]M Herajy, F Liu, C Rohr, and M Heiner. Snoopy's hybrid simulator: A tool to construct and simulate hybrid biological models. *BMC Systems Biology*, 11(1):71, Jul 2017.

[19]M Herajy, F Liu, and M Heiner. Efficient modelling of yeast cell cycles based on multisite phosphorylation using coloured hybrid Petri nets with marking-dependent arc weights. *Nonlinear Analysis: Hybrid Systems*, 27:191 – 212, 2018.

[20]D. Gillespie. Exact stochastic simulation of coupled chemical reactions. *J. Phys. Chem.*, 81(25):2340–2361, 1977.

[21]D. Gillespie. *Markov Processes: An Introduction for Physical Scientists*. Academic Press, 1991.

[22]Fei Liu, Siyuan Chen, Monika Heiner, and Hengjie Song. Modeling biological systems with uncertain kinetic data using fuzzy continuous Petri nets. *BMC Systems Biology*, 12(4):42, 2018.

[23]Fei Liu, Wujie Sun, Monika Heiner, and David Gilbert. Hybrid modelling of biological systems using fuzzy continuous Petri nets. *Briefings in Bioinformatics*, 22(1):438–450, 12 2019.

[24]Hans-Jürgen Zimmermann. *Fuzzy set theory—and its applications*. Springer Science & Business Media, 2011.

[25]Fei Liu, Monika Heiner, and David Gilbert. Fuzzy Petri nets for modelling of uncertain biological systems. *Briefings in Bioinformatics*, 21(1):198–210, 12 2018.

[26]L. Zadeh. Fuzzy sets. *Information and Control*, 8:338–353, 1965.

[27]E S Istvan, M Palnitkar, S K Buchanan, and J Deisenhofer. Crystal structure of the catalytic portion of human HMG-CoA reductase: insights into regulation of activity and catalysis. *EMBO J*, 19(5):819–830, March 2000.

[28]Stephen D Turley and John M Dietschy. The intestinal absorption of biliary and dietary cholesterol as a drug target for lowering the plasma cholesterol level. *Prev Cardiol*, 6(1):29–33, 64, 2003.

[29]Bonhi S. Bhattacharya, Peter K. Sweby, Anne-Marie Minihane, Kim G. Jackson, and Marcus J. Tindall. A mathematical model of the sterol regulatory element binding protein 2 cholesterol biosynthesis pathway. *Journal of Theoretical Biology*, 349:150–162, 2014.

[30]Bonhi S Bhattacharya, Peter K Sweby, Anne-Marie Minihane, Kim G Jackson, and Marcus J Tindall. A mathematical model of the sterol regulatory element binding protein 2 cholesterol biosynthesis pathway. *J Theor Biol*, 349(100):150–162, January 2014.

[31]Joseph L. Goldstein, Michael S. Brown, Richard G. W. Anderson, David W. Russell, and Wolfgang J. Schneider. Receptor-mediated endocytosis: Concepts emerging from the ldl receptor system. *Annual Review of Cell Biology*, 1(1):1–39, 1985.

[32]H H Hobbs, D W Russell, M S Brown, and J L Goldstein. The LDL receptor locus in familial hypercholesterolemia: mutational analysis of a membrane protein. *Annu Rev Genet*, 24:133–170, 1990.

[33]Frances Pool, Peter K. Sweby, and Marcus J. Tindall. An integrated mathematical model of cellular cholesterol biosynthesis and lipoprotein metabolism. *Processes*, 6(8), 2018.

[34]Ashish Sarraju, Andrew Ward, Jiang Li, Areli Valencia, Latha Palaniappan, David Scheinker, and Fatima Rodriguez. Personalizing cholesterol treatment recommendations for primary cardiovascular disease prevention. *Scientific Reports*, 12(1):23, Jan 2022.

[35]Yuri Efremov, Anastasia Ermolaeva, Georgiy Vladimirov, Susanna Gordleeva, Andrey Svistunov, Alexey Zaikin, and Peter Timashev. A mathematical model of in vitro hepatocellular cholesterol and lipoprotein metabolism for hyperlipidemia therapy. *PloS one*, 17(6):e0264903, 2022.